JOURNAL OF MATERIALS SCIENCE **32** (1997) 2347–2352

Structural studies of reactive pulsed laser-deposited CN_x films by X-ray photoelectron spectroscopy and infrared absorption

C. W. ONG, X.-A. ZHAO*, Y. C. TSANG, C. L. CHOY, P. W. CHAN
Department of Applied Physics and Materials Research Center, The Hong Kong Polytechnic University, Hung Hom, Kowloon, Hong Kong

The changes in the structure of reactive pulsed laser-deposited (RPLD) CN_x films with nitrogen content from 3.6–22 at% have been investigated by X-ray diffraction, X-ray photoelectron spectroscopy (XPS) and Fourier transform–infrared (FT–IR) absorption. The films were found to be amorphous, and to consist of a network of rings. The rings that were composed solely of carbon atoms gave rise to an XPS peak located between 284.3 and 284.8 eV (C^1 component). The rings containing nitrogen led to another peak located between 285.5 and 286.4 eV (C^2 component). When the nitrogen content increased, the relative intensity of the C^1 component fell, while that of the C^2 component rose, indicating that some carbon atoms in the rings were replaced by nitrogen atoms. C≡N bonds also contributed to the C^2 component. The FT–IR data were consistent with this interpretation. No evidence for the existence of a β-C_3N_4 phase was found in RPLD CN_x films.

1. Introduction

There has been considerable interest in the synthesis of carbon nitride (CN_x), since it was predicted that a β-C_3N_4 phase with a hardness comparable with that of diamond, may exist [1, 2]. However, no one has successfully prepared CN_x with a high nitrogen content (57 at%) as predicted for the β-C_3N_4 phase [3–21]. In the preparation techniques employed so far, such as particle-beam-assisted laser processing [3–6], dual-ion-beam deposition [7–10], electron cyclotron resonance [11], reactive sputtering [12–18], ion-assisted evaporation [19] and nitrogen implantation [20], energetic particle bombardments were generally involved, so the lack of nitrogen was attributed to the preferential sputtering of nitrogen [8, 10, 18], thereby preventing the formation of a β-C_3N_4 phase. However, in a recent study on reactive pulsed laser-deposited (RPLD) CN_x films, it was found that even when energetic particle bombardments are absent, and selective sputtering of nitrogen is negligible, the nitrogen content in the films is still low [21]. This result suggests that there are other factors limiting the nitrogen incorporation into the films. Therefore, it is of great interest to investigate how the structure of CN_x films changes when the nitrogen content increases. In this article, we present the results of a study of the structure of RPLD CN_x films as a function of nitrogen content using X-ray diffraction (XRD), X-ray photoelectron spectroscopy (XPS) and Fourier transform–infrared absorption (FT–IR). In particular, to interpret the results of the XPS measurements, we fitted the C 1s peaks by referring to the published data of some related materials as a guideline. Furthermore, the XPS data of CN_x films reported by some other groups were also collected and discussed.

2. Experimental procedure

In this study, the CN_x samples were prepared by reactive pulsed laser deposition. The preparation system was described in detail elsewhere [21, 22]. The deposition processes were performed in a stainless steel chamber evacuated by a diffusion pump to a background pressure $< 5 \times 10^{-5}$ torr (1 torr = 133.322 Pa). The second harmonic from a *Q*-switched Nd–YAG laser with a wavelength of 532 nm was focused by a quartz lens on to a graphite rod. The graphite rod was rotated and moved back and forth during deposition to prevent the formation of craters. The laser power density was fixed at 9.2×10^8 W cm^{-2}. Nitrogen gas (purity > 99.995%) was admitted into the chamber by a mass flow controller (MKS Model 1259C). The flow rate was fixed at 20 standard cm^3 min^{-1}, and the nitrogen partial pressure, P_{N_2}, was varied from 5–300 m torr by adjusting a butterfly vacuum valve. A (1 0 0) silicon substrate was mounted at a distance of about 4 cm from the target. Within the experimental range of P_{N_2}, the mean free path of the particles in the gas was shorter than the substrate/target distance, such that any energetic

---

* *Permanent address*: Shanghai Research Institute of Materials, Shanghai, People's Republic of China.

particles, including the laser-ablated carbon species ejected from the target, would be thermalized and slowed down before reaching the substrate surface. As a result, preferential sputtering of nitrogen from the growing film was negligible.

The film thickness, measured by an α-step depth profiler (Tencor 100), varied between 570 and 1450 nm. The XRD experiment was performed by using a Philips X'PERT System. The results show that all the samples were amorphous. For XPS analyses, a Kratos Analytical System equipped with a $\mathrm{Mg}K_\alpha$ 1253.6 eV X-ray source was used. Before performing the XPS experiment, the sample was first cleaned by a 4 keV argon ion beam for 10 min. The Shirley method was used to subtract the background from the XPS spectra [23]. After subtracting the background, the peak energy was determined by referring to the Au 1s peak at 83.98 eV. The atomic fraction of nitrogen in the films, defined as $F = [\mathrm{N}]/([\mathrm{N}] + [\mathrm{C}])$, was evaluated by using the expression

$$F = \left(\frac{A_\mathrm{N}}{0.42}\right) \Big/ \left(\frac{A_\mathrm{C}}{0.25} + \frac{A_\mathrm{N}}{0.42}\right) \qquad (1)$$

where A_N and A_C are the areas under the N 1s and C 1s peaks, and the constants 0.42 and 0.25 are the sensitivity factors of nitrogen and carbon, respectively. The values of F were found to vary from 0.036–0.22 as P_{N_2} increased from 5–300 m torr. The infrared absorption spectra of the films were obtained from 500–4000 cm^{-1} using a Nicolet's Magna-TR™ System 750.

3. Results

Fig. 1a and b show the carbon XPS spectra of the samples deposited at $P_{\mathrm{N}_2} = 5$ and 300 m torr, respectively, and Fig. 2a and b show the corresponding C 1s peaks after the backgrounds have been subtracted. We see from Fig. 2 that, as F increases, the C 1s peak becomes broader and more asymmetrical, and the peak position moves towards higher binding energy.

We first note that the C 1s peak of graphite is also asymmetrical. The peak has a tail located on the higher energy side, which was suggested to be induced by the delocalized π bonds [24, 25]. Warner *et al.* [24] first characterized the asymmetry of highly oriented pyrolytic graphite (HOPG) and hydrogenated amorphous carbon (a-C : H) by a parameter, α. A Gaussian curve was used to fit the lower energy side of the C 1s spectrum, and then α was taken to be $(A_\mathrm{exp} - A_\mathrm{G})/A_\mathrm{G}$, where A_exp and A_G are the areas under the observed curve and the Guassian curve, respectively. For HOPG, α was found to be about 0.25, whereas a-C : H had lower α values (0.0075–0.15).

To check whether the broadening of the C 1s peak of our samples arises from the same cause, we followed the procedure of Warner *et al.* [24], and found that the α values (0.45–0.82) of our samples were much higher than those of HOPG and a-C : H. Therefore, we believe that the broadening of the C 1s peak of our samples was not due to the π electrons. After excluding this possibility, we analysed the C 1s peak by referring to the XPS data of two groups of related materials. The first group, which includes graphite and benzene, is composed of rings of carbon atoms, and have C 1s peaks with energy ≤ 284.8 eV. The other group includes the materials containing carbon and nitrogen atoms. The C 1s peaks of these materials have higher energies owing to the charge transfer resulting from the incorporation of nitrogen, which is more electronegative than carbon. As a simple model, the C 1s peak of our samples is assumed to consist of two components, C^1 and C^2, which are attributed to the pure carbon rings and the chemical bonds associated with nitrogen, respectively. A Gaussian curve is used to describe each component. Then the peak positions and peak widths of the two Gaussian curves are adjusted to give a least-squares fit to the data. As

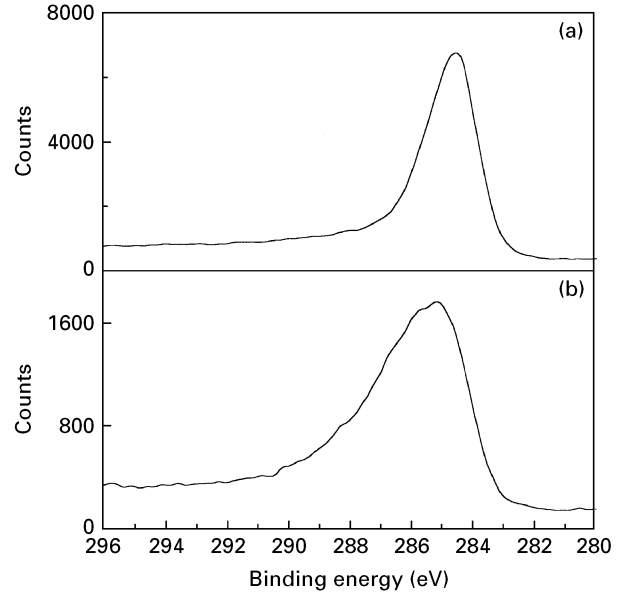

Figure 1 The carbon XPS spectra of the samples deposited at P_{N_2} of (a) 5 m torr ($F = 0.036$), and (b) 300 m torr ($F = 0.22$) .

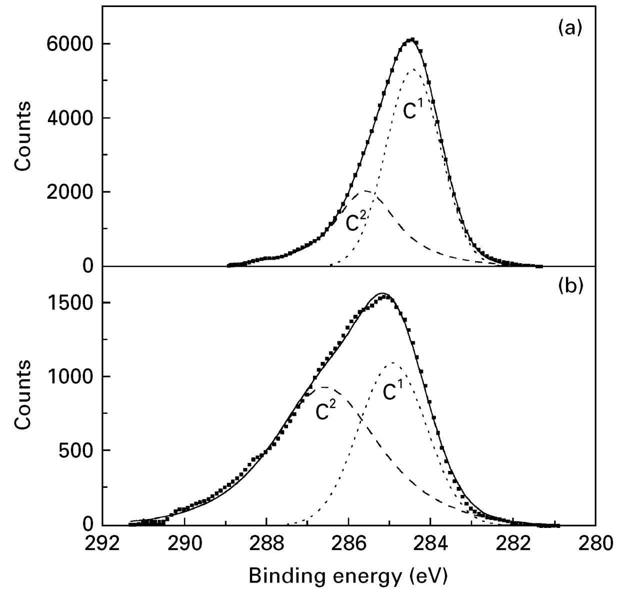

Figure 2 The XPS spectra of C 1s peak after subtracting the background. (a) $P_{\mathrm{N}_2} = 5$ m torr ($F = 0.036$), and (b) $P_{\mathrm{N}_2} = 300$ m torr ($F = 0.22$). (——) $\mathrm{C}^1 + \mathrm{C}^2$.

examples of the results of fitting, the components for two samples are shown in Fig. 2a and b. We note that Mansour and Ugolini [26] have previously used a similar model to fit the C 1s peak of a-CN_x : H films, and have assigned the Gaussian curve at low binding energy to the carbon atoms surrounded by carbon and hydrogen atoms, and the Gaussian curve at high binding energy to the carbon atoms surrounded by nitrogen, carbon and hydrogen atoms.

Fig. 3 shows that, as F increases from 0.036 to 0.22, there is a slight shift in the peak position of the C^1 component, but the peak lies within the range 284.3–284.8 eV. This covers the range of C 1s peak positions of graphite and benzene reported by various groups [7, 11, 12, 26–31], so the result is consistent with our assumption that the C^1 component is associated with pure carbon rings.

On the other hand, the peak position of the C^2 component falls within 285.5–286.4 eV. Comparing with the energies of the C 1s peaks of the related well-known compounds, we first found that pyridine (C_5H_5N), a molecule consisting of an aromatic ring with one nitrogen atom at the sp^2 site, has a peak at 285.5 eV [9, 26, 32]. This indicates that the C^2 component partly arises from rings containing nitrogen atoms. Secondly, the energy of the C^2 component is also close to that of the C≡N triple bonds of benzonitrile (Ph–C*≡N) at 285.4 eV [33], suggesting that C≡N groups may also exist in the films. Furthermore, the C^2 component may also include the contribution from C–C groups similar to those in acetonitrile (H_3C^*–C≡N), which lead to a peak at 286.3 eV [32].

The fractions of the C^1 and C^2 components were obtained by calculating the areas under the curves. As shown in Fig. 4, when the nitrogen content increases, the relative fraction of the C^1 component drops, while that of the C^2 component rises. This is because the number of the rings consisting of pure carbon decreases, while the number of chemical bonds containing nitrogen increases.

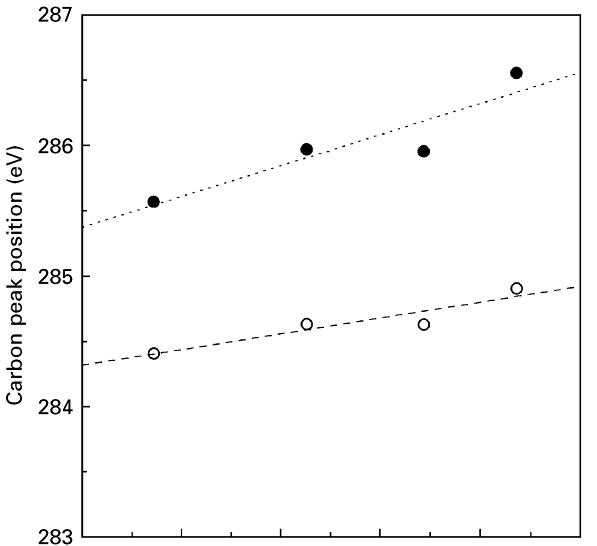

Figure 3 The peak positions of the (○) C^1 and (●) C^2 components versus atomic fraction of nitrogen.

Fig. 5 shows the dependence of the peak width of the two components on the nitrogen content. The full-width at half-maximum (FWHM) of the C^1 component shows a slight increase (from 1.6 eV to 1.9 eV) as F increases from 0.036 to 0.22. Because the C^1 component is believed to be associated with the carbon rings in the films, it is natural to attribute the broadening of this component to the increase of disorder of the bond length and bond angle within a carbon ring. In order to estimate the magnitude of the broadening due to a similar kind of disorder, the FWHM of the C 1s peak of graphite and a-C : H were

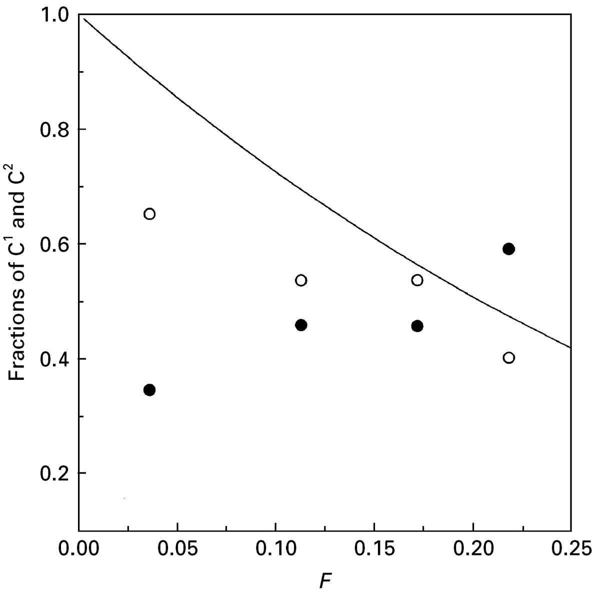

Figure 4 The relative fractions of the (○) C^1 and (●) C^2 components versus atomic fraction of nitrogen. (——) The prediction obtained from a simple model (see text).

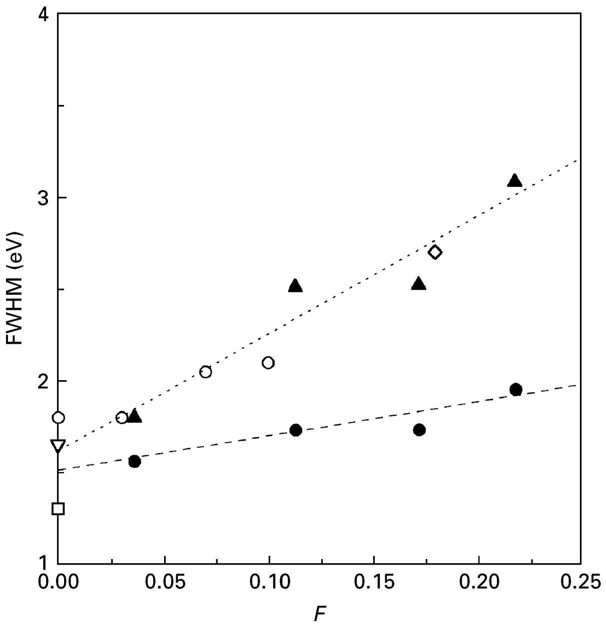

Figure 5 The full-width at half-maximum of the (●) C^1 and (▲) C^2 components versus atomic fraction of nitrogen: (□) graphite [25], (▽) a-C : H prepared by ionized deposition of methane [27], (○) a-C : H and a-CN : H prepared by ion-beam deposition [26], (◇) CN_x films deposited by dual-ion-beam technique [7], (▲, ●) present data.

calculated from published XPS spectra, and found to be about 1.3 and 1.8 eV, respectively [25–27]. The fact that the data for our samples fall within the above range (see Fig. 5) provides further confirmation that the broadening of the C^1 component is due to the higher disorder within the carbon rings.

It is also seen from Fig. 5 that the FWHM of the C^2 component exhibits a pronounced increase with increasing nitrogen content. Because this component is believed to be associated with the groups containing nitrogen atoms, we suggest that the broadening is due to the disorder of bond length and bond angle of the chemical bonds associated with the incorporated nitrogen atoms. To check the influence of the nitrogen atoms on the peak width, we calculated the FWHM of the overall C 1s peak from the published XPS spectra of CN_x films prepared by other techniques [7, 26]. The results obtained are plotted in Fig. 5, which show a trend similar to that of the FWHM of the C^2 component of our samples, indicating that the broadening of this component is probably caused by the disorder of nitrogen-related chemical bonds. We also note that the broadening effect of this component is rather insensitive to the preparation processes employed, but depends mainly on the nitrogen content in the films.

The results of FT–IR experiments are shown in Fig. 6. For the pure carbon sample ($F = 0$), three absorption bands (bands I, II and III) are barely observed. When the nitrogen content increases, the intensities of all three bands increase. In particular, bands II and III grow remarkably even when a small amount of nitrogen, e.g. $F = 0.036$, is incorporated. Similar absorption bands of CN_x films were reported by other workers, who associated the bands with the vibrational modes of the graphite structure (see Table I). Bands I and III were assigned to the out-of-plane bending modes [15, 21] and in-plane vibrational modes (E_{2g} symmetry) [15, 16, 20, 21] of the graphite-like sp^2 domains, respectively, and band II to the in-plane vibrational modes at the surface of the sp^2 domains [15, 16, 21]. To explain the rapid growth of bands II and III, we first note that the vibrational modes of pure carbon rings are IR forbidden (but Raman active) [16]. When nitrogen atoms are incorporated into the films, they replace some of the carbon atoms and disrupt the symmetry of the hexagonal atomic rings, thereby giving rise to IR active vibrational modes. Moreover, band IV appears at 2200 cm^{-1}. This band is associated with the stretching mode of C≡N [11, 12, 15, 21, 34].

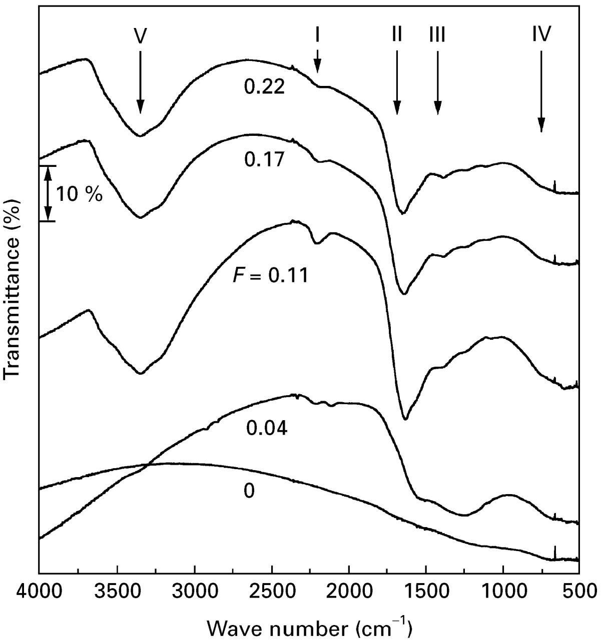

Figure 6 The Fourier transform-infrared absorption spectra of RPLD CN_x films.

The FT–IR data are consistent with the interpretations derived from the XPS experiment, which indicate the existence of pure carbon rings, the replacement of carbon atoms in the rings by incorporated nitrogen, and the formation of C≡N triple bonds in RPLD CN_x films.

Finally, we observed a band at 3300 cm^{-1}, which may be attributed to the stretching mode of NH_2 bonds [21, 34]. However, the origin of hydrogen in the present experiment is still not known.

4. Discussion

To date, there is no consensus on the structure of CN_x films. This may be due to the difference in deposition methods, or the limitations of diagnostic techniques. The results of the present study suggest that RPLD CN_x films are graphitic and contain C≡N bonds, consistent with the model proposed by Wood *et al.* [34] for CN_x films prepared by r.f. plasma decomposition of a mixture of hydrocarbon vapor and nitrogen gas. CN_x films prepared by other techniques, such as ion-assisted pulsed laser deposition, ion-beam deposition, d.c. magnetron sputtering, electron cyclotron resonance and ion-assisted electron-beam evaporation [4, 9, 11], were found to contain a certain fraction of graphitic structure. The related XPS data are collected and discussed below.

It has been claimed that there is evidence for the existence of sp^3 bonds in CN_x films, which is the necessary condition for the formation of a β-C_3N_4

TABLE I Infrared absorption bands of CN_x films

	Observed IR bands	Assignments	Reference
I	Below 840 cm^{-1}, minimum ~670 cm^{-1}	Graphite-like sp^2 domains	[15, 21]
II	1200–1450 cm^{-1}, minimum ~1300 cm^{-1}	Disordered sp^2 domains	[15, 16, 21]
III	1500–1750 cm^{-1}, minimum ~1600 cm^{-1}	Graphite-like sp^2 domains	[15, 16, 21]
IV	2200 cm^{-1}	C≡N	[11, 12, 15, 21, 34]
V	2900–3600 cm^{-1}, minimum ~3300 cm^{-1}	NH_2	[21, 34]

phase. Niu *et al.* and Song *et al.* associated their C 1s peaks at 284.6 [5] and 285.8 eV [7] with the diamond peak, which led them to suggest that sp^3 bonds were present in their CN_x films. However, because the reported positions of the C 1s peak of diamond are widely scattered between 284.3 and 287.28 eV [5, 7, 11, 27, 28, 35], it is uncertain which peak position should be chosen as an indication of sp^3 bonds. Similarly, Ren *et al.* and Marton *et al.* correlated their C 1s peaks at 286.9 [4] and 287.7 eV [9], respectively, with the carbon atoms located at sp^3 sites. In particular, Marton *et al.* [9] referred their peak to that of urotropine ($(CH_2)_6N_4$) at 286.9 eV, a molecule in which the carbon atoms have sp^3 bonds. However, one notices that the C 1s peak of the C≡N bond in acetonitrile ($H_3C–C^*≡N$) is located at 287.2 eV [32], which is very close to the peaks reported by Ren *et al.* [4] and Marton *et al.* [9]. Finally, it should be pointed out that all of the above C 1s peaks which have been assigned to sp^3 bonds lie in a range as broad as 3.1 eV. Therefore, we suggest that more experiments other than XPS need to be carried out in order to identify the β-C_3N_4 phase.

The N 1s peak, located around 399 eV (Table II), is broad (FWHM $\approx$ 3.3 eV). Because the shape of the peak is almost independent of F, it is difficult to suggest a curve-fitting procedure based on visual inspection. It is also difficult to obtain structural information by referring to the N 1s peaks of related materials. As summarized in the third column of Table II, the nitrogen atoms in the following chemical groups give N 1s peaks in the energy range between 398.8 and 404 eV:

(i) N≡N in nitrogen gas molecule (399–404 eV) [7, 11, 12, 19, 20, 28, 36];

(ii) pyridine molecule (398.8–400.5 eV) [9, 26, 32, 37, 38];

(iii) C=N in *N*-benzylideneaniline [39], C≡N in benzonitrile [37], C–N in aniline [37], sp^2 bonds in urotropine [9, 37], and N=N in *trans*-azobenzene [37, 40] (399.1–400.1 eV).

The N 1s peaks for CN_x films reported by various authors are listed in the second column of Table II for reference. Possibly because of the difficulty in fitting the N 1s peak, or finding correlation between the peak energies and chemical bonds, most of these data have been reported without detailed interpretation.

With the aid of a simple model, it is possible to find the fraction of the C^1 component from the atom fraction of nitrogen, F. Consider an infinite graphitic network composed of carbon and nitrogen atoms. A particular carbon atom in this network may be surrounded by three carbon atoms, or two carbon atoms and one nitrogen atom, or one carbon atom and two nitrogen atoms, or three nitrogen atoms. The probability for the first case, $(1 - F)^3$, should be equal to the fraction of the C^1 component. Although the curve $y = (1 - F)^3$ does not agree exactly with the experimental data, it reproduces the F dependence of the fraction of the C^1 component reasonably well (see Fig. 4). The discrepancy between the theoretical prediction and the experimental data can be attributed to the existence of disorder, defects and clusters in the graphitic network.

5. Conclusion

In conclusion, both the results of XPS and FT–IR analyses of RPLD CN_x films indicate that the structure of the samples is graphitic. By fitting the C 1s peak, we can estimate the relative fraction of rings of carbon atoms and the chemical bonds containing nitrogen, such as the bonds in nitrogenated rings and C≡N bonds. With increasing nitrogen content, the relative fraction of pure carbon rings drops, while the chemical groups containing nitrogen increases. The incorporation of nitrogen leads to a weakening of the mechanical strength [21]. There is no evidence for

TABLE II Energies of N 1s peaks for CN_x films and some related materials containing carbon and nitrogen

Energy (eV) Present work	Other work (eV)	N 1s peaks of related materials
	397.4 covalent carbon nitride structure [4]	
	398.0 [20]	
	398.3 associated with β-C_3N_4 [9]	
	398.5 [19]	
	398.6 [11]	
	398.9 [7, 20]	
		398.8 C_5H_5N (pyridine) [37]
399	399.0 [3]	399 nitrogen [7, 12, 28]
Width ≈3.3 eV	399.1 [4, 5]	399.1 PhCH=NPh (*N*-benzylideneaniline) [39]
	399.2 [12]	399.2 PhC≡N (benzonitrile) [37]
		399.3 nitrogen [11] C_5H_5N (pyridine) [32]
		399.4 $PhNH_2$ (aniline) [37] $(CH_2)_6N_4$ (urotropine) [9, 37]
	399.5 [26]	399.5 nitrogen [19]
		399.6 PhN=NPh (*trans*-azobenzene) [40]
		399.8 C_5H_5N (pyridine) [9, 38]
	400.0 associated with pyridine [9]	
	400.1 [20]	400.1 PhN=NPh (*trans*-azobenzene) [37]
		400.5 C_5H_5N (pyridine) [26]
		404 physisorbed N_2 on graphite [20, 36]

the formation of a β-C_3N_4 phase in RPLD CN_x films.

Acknowledgements

We thank Dr R. W. M. Kwok and G. L. Jin, Chinese University of Hong Kong, for their help in the XPS analyses. The work also obtained the financial support from the Hong Kong Polytechnic University under the Code nos. 0420-031-00-110 and 0350-362-A3-110.

References

1. A. Y. LIU and M. L. COHEN, *Phys. Rev. B* **41** (1990) 10727.
2. *Idem, Science* **245** (1989) 841.
3. Z. M. REN, Y. C. DU, Z. F. YING, Y. X. QUI, X. X. XIONG, J. D. WU and F. M. LI, *Appl. Phys. Lett.* **65** (1994) 1361.
4. Z. M. REN, Y. C. DU, Y. X. QUI, J. D. WU, Z. F. YING, X. X. XIONG and F. M. LI, *Phys. Rev. B* **51** (1995) 5274.
5. C. NIU, Y. Z. LU and C. M. LIEBER, *Science* **261** (1993) 334.
6. J. NARAYAN, J. REDDY, N. BIUNNO, S. K. KANETKAR, P. TIWARI and N. PARIKH, *Mater. Sci. Eng. B* **26** (1994) 49.
7. H. W. SONG, F. Z. CUI, X. M. HE, W. Z. LI and H. D. LI, *J. Phys. Condens. Matter* **6** (1994) 6125.
8. D. MARTON, A. H. AL-BAYATI, S. S. TODOROV, K. J. BOYD and J. W. RABALAIS, *Nucl. Instrum. Meth. B* **90** (1994) 277.
9. D. MARTON, K. J. BOYD, A. H. AL-BAYATI, S. S. TODOROV and J. W. RABALAIS, *Phys. Rev. Lett.* **73** (1994) 118.
10. H. C. HOFSÄSS, C. RONNING, U. GRIESMEIER and M. GROSS, *Mater. Res. Soc. Symp. Proc.* **354** (1995) 93.
11. A. BOUSETTA, M. LU, A. BENSAOULA and A. SCHULTZ, *Appl. Phys. Lett.* **65** (1994) 696.
12. S. KUMAR and T. L. TANSLEY, *Solid State Commun.* **88** (1993) 803.
13. *Idem, J. Appl. Phys.* **76** (1994) 4390.
14. K. M. YU, M. L. COHEN, E. E. HALLER, W. L. HANSEN, A. Y. LIU and I. C. WU, *Phys. Rev. B* **49** (1994) 5034.
15. N. NAKAYAMA, Y. TSUCHIYA, S. TAMADA, K. KOSUGE, S. NAGATA, K. TAKAHIRO and S. YAMAGUCHI, *Jpn J. Appl. Phys.* **32** (1993) L1465.
16. J. H. KAUFMAN, S. METIN and D. D. SAPERSTEIN, *Phys. Rev. B* **39** (1989) 13053.
17. J. J. CUOMO, P. A. LEARY, D. YU, W. REUTER and M. FRISCH, *J. Vac. Sci. Technol.* **16** (1979) 299.
18. H. SJÖSTRÖM, I. IVANOV, M. JOHANSSON, L. HULTMAN, J.-E. SUNDGREN, S. V. HAINSWORTH, T. F. PAGE and L. R. WALLENBERG, *Thin Solid Films* **246** (1994) 103.
19. J. F. D. CHUBACI, T. SAKAI, T. YAMAMOTA, K. OGATA, A. EBE and F. FUJIMOTO, *Nucl. Instrum. Meth. B* **80/81** (1993) 463.
20. A. HOFFMAN, I. GOUZMAN and R. BRENER, *Appl. Phys. Lett.* **64** (1994) 845.
21. X.-A. ZHAO, C. W. ONG, Y. C. TSANG, Y. W. WONG, P. W. CHAN and C. L. CHOY, *ibid.* **66** (1995) 2652.
22. C. W. ONG, X.-A. ZHAO, J. T. CHEUNG, S. K. LAM, Y. LIU, C. L. CHOY and P. W. CHAN, *Thin Solid Films* **258** (1995) 34.
23. G. C. SMITH, "Surface Analysis by Electron Spectroscopy" (Plenum Press, New York, 1994) p. 45.
24. J. D. WARNER, J. J. POUCH, S. A. ALTEROVITZ, D. C. LIU and W. A. LANFORD, *J. Vac. Sci. Technol. A* **3** (1985) 900.
25. T. T. P. CHEUNG, *J. Appl. Phys.* **53** (1982) 6857.
26. A. MANSOUR and D. UGOLINI, *Phys. Rev. B* **47** (1993) 10201.
27. T. MORI and Y. NAMBA, *J. Appl. Phys.* **55** (1984) 3276.
28. F. FUJIMOTO and K. OGATA, *Jpn J. Appl. Phys.* **32** (1993) L420.
29. G. JOHANSSON, J. HEDMAN, A. BERNDTSSON, M. KLASSON and R. NILSSON, *J. Electron Spectrosc. Relat. Phenom.* **2** (1973) 295.
30. J. F. MOULDER, W. F. STICKLE, P. E. SOBOL and K. D. BOMBEN, "Handbook of X-ray Photoelectron Spectroscopy", edited by J. Chastain (Perkin-Elmer Corporation, Eden Prairie, 1992) p. 216.
31. U. GELIUS, P. F. HEDEN, J. HEDMAN, B. J. LINDBERG, R. MANNE, R. NORDBERG, C. NORDLING and K. SIEGBAHN, *Phys. Scripta* **2** (1970) 70.
32. M. BARBER, J. A. CONNOR, M. F. GUEST, I. H. HILLIER, M. SCHWARZ and M. STACEY, *J. Chem. Soc. Farad. Trans. II* **69** (1973) 551.
33. R. LARSSON and B. FOLKESSON, *Chem. Scripta* **9** (1976) 148.
34. P. WOOD, T. WYDEVEN and O. TSUJI, *Thin Solid Films* **258** (1995) 151.
35. D. N. BELTON, S. T. HARRIS, S. J. SCHMIEG, A. M. WEINER and T. A. PERRY, *Appl. Phys. Lett.* **54** (1989) 416.
36. A. NILSON, O. BJORNEHOLM, H. TILLBORG, B. HERNNAS, R. J. GUEST, A. SANDELL, R. E. PALMER and N. MARTENSSON, *Surf. Sci.* **287/288** (1993) 758.
37. B. J. LINDBERG and J. HEDMAN, *Chem. Scripta* **7** (1975) 155.
38. H. BOEHLAND, W. HANAY, A. MEISEL and R. SCHEIBE, *Z. Chem.* **10** (1981) 372.
39. J. V. SALYN, E. K. ZUMADILOV, V. I. NEFEDOV, R. SCHEIBE, G. LEONHARDT, L. BEYER and E. Z. HOYER, *Anorg. Allg. Chem.* **432** (1977) A275.
40. P. BRANT and R. D. FELTHAM, *J. Organometal. Chem. C* **53** (1976) 120.

Received 25 March
and accepted 3 October 1996